SCIENTIFIC REP⚙RTS

Interfacial exchange coupling and magnetization reversal in perpendicular [Co/Ni]$_N$/TbCo composite structures

M. H. Tang[1], Zongzhi Zhang[1], S. Y. Tian[2], J. Wang[2], B. Ma[1] & Q. Y. Jin[1]

Interfacial exchange coupling and magnetization reversal characteristics in the perpendicular heterostructures consisting of an amorphous ferrimagnetic (FI) Tb$_x$Co$_{100-x}$ alloy layer exchange-coupled with a ferromagnetic (FM) [Co/Ni]$_N$ multilayer have been investigated. As compared with pure Tb$_x$Co$_{100-x}$ alloy, the magnetization compensation composition of the heterostructures shift to a higher Tb content, implying Co/Ni also serves to compensate the Tb moment in TbCo layer. The net magnetization switching field $H_{c\perp}$ and interlayer interfacial coupling field H_{ex}, are not only sensitive to the magnetization and thickness of the switched Tb$_x$Co$_{100-x}$ or [Co/Ni]$_N$ layer, but also to the perpendicular magnetic anisotropy strength of the pinning layer. By tuning the layer structure we achieve simultaneously both large $H_{c\perp} = 1.31$ T and $H_{ex} = 2.19$ T. These results, in addition to the fundamental interest, are important to understanding of the interfacial coupling interaction in the FM/FI heterostructures, which could offer the guiding of potential applications in heat-assisted magnetic recording or all-optical switching recording technique.

In the past years, extensive work has been devoted to the heterostructures with a ferromagnetic (FM) /antiferromagnetic (AFM) exchange coupling interface[1–6]. The exchange bias effect[7], arising from the interfacial unidirectional anisotropy and displaying a shift along the magnetic field axis of the magnetic hysteresis loop, has been employed in giant magnetoresistance (GMR) devices for magnetic data storage applications[8–10]. Recently, with great demand for increasing storage density, new writing technique such as heat-assisted magnetic recording (HAMR)[10–12] and all-optical switching (AOS)[13,14] have received much attention, which intrigues great interest in seeking perpendicular exchange-coupled heterostructures with strong and temperature (*T*) sensitive interfacial AFM exchange coupling. However, in previous studies, most of the exchange-coupled heterostructures with perpendicular magnetic anisotropy (PMA) are restricted to a FM layer antiferromagnetically coupled with an AFM layer such as MnIr or FeMn, for which the room temperature (RT) coupling field (H_{ex}) is usually below 0.1 T[3–6], apparently cannot meet the practical requirements of future high density data storage.

It is known that in ferrimagnetic (FI) rare earth-transition metal (RE-TM) alloy films, there are two types of pair interactions: antiparallel exchange between the RE-TM moments and parallel exchange of the TM moments themselves, both interactions would greatly enhance the coupling strength[12,14–18]. Moreover, amorphous ferrimagnetic RE-TM films such as TbCo or TbFe can exhibit strong PMA when the antiferromagnetically coupled magnetic moments of RE and TM are nearly balanced by controlling the element composition or measurement temperature[19]. As a result, a perpendicular heterostructure consisting of a FM layer in contact with a FI alloy layer can owns not only low stray field, but also strong,

[1]Shanghai Engineering Research Center of Ultra-precision Optical Manufacturing, and Key Laboratory of Micro and Nano Photonic Structures (Ministry of Education), Department of Optical Science and Engineering, Fudan University, Shanghai, 200433, China. [2]Department of Physics, Ningbo University, Ningbo 315211, China. Correspondence and requests for materials should be addressed to Z.Z. (email: zzzhang@fudan.edu.cn)
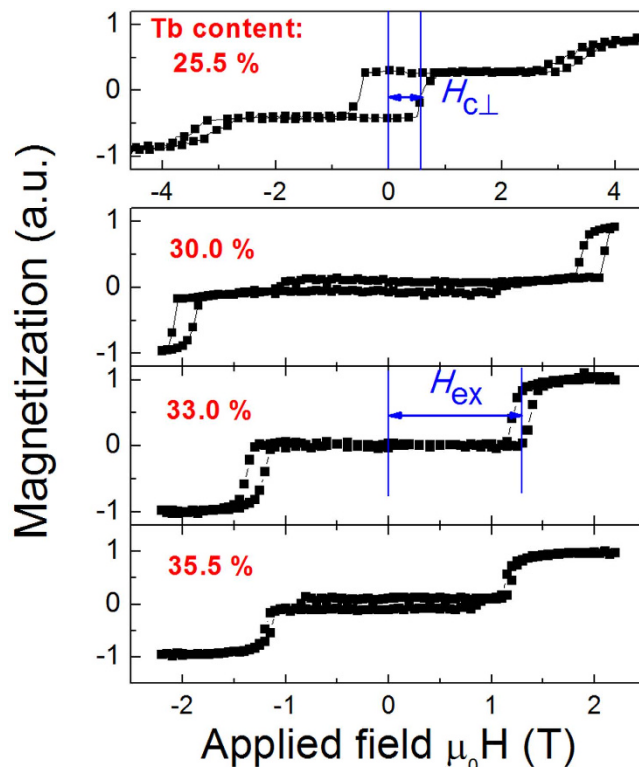
Figure 1. Magnetic hysteresis loops of different Tb contents. The out-of-plane magnetic hysteresis loops measured by PPMS for samples of $[Co0.28/Ni0.58]_5/ Tb_xCo_{100-x}$ (12) with various Tb contents, in which the $H_{c\perp}$ and H_{ex} are defined.

tunable, and T-dependent interfacial coupling and net magnetization switching fields $(H_{c\perp})$[20,21]. Such FI-based heterostructures might possess potential applications in HAMR and AOS, since its large and temperature-sensitive $H_{c\perp}$ and H_{ex} can be used to store information while the strongly coupled FM layer can improve the properties of readout. Therefore, understanding and clarifying the related coupling and switching mechanism in the FM/FI heterostructures should be of great importance for ultrahigh density recording in these new storage techniques.

Due to the great potential applications in data storage technology, in recent years some research work has been performed regarding the FM/FI composite structures[12,15–17]. For instance, S. Romer *et al.* investigated the temperature dependence of large exchange bias effect in TbFe/[Co/Pt] system[12]. The dependence of interfacial exchange coupling on the stoichiometry of TbFe layer and repetition numbers of Co/Pt was analyzed by C. Schubert *et al.*[17]. However, the net magnetization switching properties were not well analyzed in these studies. Moreover, except Co/Pt (Pd) multilayer, no other FM layer material has been employed. In our previous work, the $[Co/Ni]_N$ multilayer has been employed to couple with TbCo as the reference layer of perpendicular spin valves, by which we have achieved high GMR signal and large switching plateau[20]. The Co/Ni multilayer, which owns relatively higher spin polarization and smaller Gilbert damping factor than Co/Pt, has been considered as a potential material in MRAMs for high spin torque efficiency[22]. In order to thoroughly understand the interfacial exchange coupling, magnetization reversal, and their relationship in FM/FI heterostructures, in this work we have fabricated several series of samples of glass /Ta(3) /Cu(3) /[Co(0.28)/Ni(0.58)]$_N$ /Co(t_{Co}) /Tb$_x$Co$_{100-x}$(t) /Ta(5) (layer thickness in unit of nm). The influences of Tb contents x, Co/Ni repetition number N, and thicknesses (t_{Co} and t) of the additional Co and TbCo layers will be discussed. Note that for all these samples the easy axes of both the FI TbCo and FM [Co/Ni]$_N$ layers are maintained perpendicular to the film plane.

Results

Figure 1 displays the out-of-plane magnetic hysteresis loops measured by Physical Property Measurement System (PPMS) for the heterostructure samples of [Co/Ni]$_5$/Tb$_x$Co$_{100-x}$ (12) with various Tb content x. As defined in the loops, the magnetic coercivity $H_{c\perp}$ in the central loop corresponds to the total net magnetic moment switching, while the antiferromagnetic coupling field H_{ex} denotes the magnetization switching of either TbCo or Co/Ni layer that has lower magnetic moment. Clearly, for different x the loops exhibit different H_{ex} and $H_{c\perp}$. Especially for $x = 33.0\%$, no central switching loop can be detected,
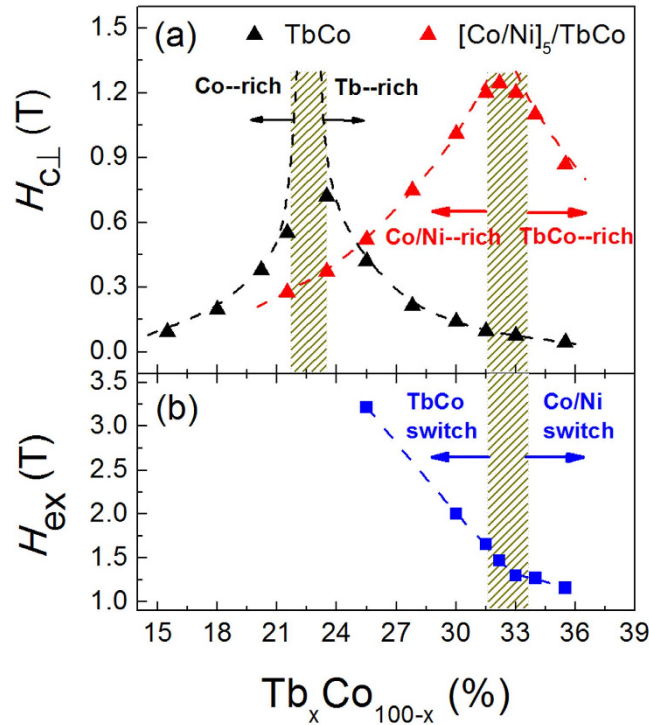
Figure 2. The Tb content influence on the $Hc_\perp$ and H_{ex}. The Tb content dependences of perpendicular coercive field $H_{c\perp}$ (**a**) and exchange coupling field H_{ex} (**b**) for the heterostructure samples of [Co0.28/ Ni0.58]$_5$/ Tb$_x$Co$_{100-x}$ (12). The $H_{c\perp}$ values for pure TbCo alloy are also shown in (**a**).

indicating that the magnetization of 12-nm thick Tb$_{33}$Co$_{67}$ layer is balanced with that of Co/Ni and thus the sample has nearly zero net magnetic moment.

In order to clearly see the variation trends, Tb content dependence of $H_{c\perp}$ and H_{ex} are shown in Fig. 2, the $H_{c\perp}$ values of pure Tb$_x$Co$_{100-x}$ are also given for comparison. Note that, for the pure TbCo alloy film, the $H_{c\perp}$ firstly increases with increasing Tb content, at $x \approx 22\%$ it starts to decrease. It is noticed that the largest $H_{c\perp}$ occurs when the magnetic moments of Tb and Co are approaching compensated according to the inverse relation to the magnetization[23],

$$H_{c\perp} \approx K_{eff}/M_{net} \tag{1}$$

where K_{eff} and M_{net} denote the effective magnetic anisotropy and net saturation magnetization of the heterostructure, respectively. As a result, for our 12-nm thick TbCo film, the magnetization compensation composition at RT is approximately 22%. Interestingly, for the perpendicularly exchange-coupled [Co/ Ni]$_5$/TbCo composite film, a similar relationship between Tb content and $H_{c\perp}$ happens. Nevertheless, the RT compensation composition has been moved to a higher Tb content of $x \approx 33\%$, verifying that the Co/Ni atoms also serve to compensate the magnetic moment of Tb atoms in the Tb-rich TbCo layer[20,21]. Therefore, for $x < 33\%$, the heterostructure is [Co/Ni]$_5$ rich in magnetic moment and the H_{ex} comes from magnetization switching of the TbCo layer. On the contrary, for $x > 33\%$ it becomes TbCo rich and the H_{ex} corresponds to the switching field of Co/Ni multilayer. As shown in Fig. 2(b), the H_{ex} reaches a value as high as 3.22 T at $x = 25.5\%$, significantly larger than the exchange field observed in normal FM/AFM systems. With the increase of x, it firstly decreases rapidly until x reaches the compensation point, after that it becomes nearly stable. The observed H_{ex} tendency of the heterostructure can be well interpreted by the following formula[17,24],

$$H_{ex} = \frac{J_{ex}}{M_s t} \propto \frac{K_p}{M_s t} \tag{2}$$

where J_{ex} is the interlayer coupling strength, M_s and t represent the saturation magnetization and thickness of the switched layer, while K_p is the magnetic anisotropy energy of the pinning layer, respectively. At $x < 33\%$, the TbCo layer is switched since it has a lower moment than the Co/Ni layer, so the strong decrease of H_{ex} with the increase of x is mainly caused by the increased magnetization of TbCo layer.
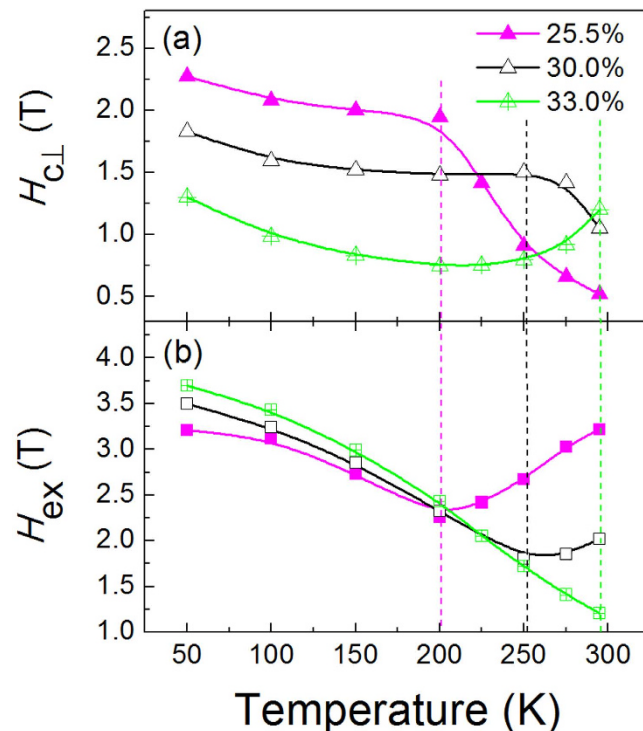
Figure 3. Temperature dependence of $Hc_\perp$ and H_{ex}. (a) The perpendicular coercive field $H_{c\perp}$ and (b) exchange coupling field H_{ex} as a function of measurement temperature for Tb contents of $x = 25.5\%$, 30.0%, and 33.0%.

At $x > 33\%$, the Co/Ni layer is switched, further increase of Tb content will only affect the K_p of TbCo slightly[25], thus giving rise to the observed slight reduction of H_{ex}.

Considering that the Tb moment enlarges much more rapidly than the transition metal as the measurement temperature decreases, the $H_{c\perp}$ and H_{ex} will have different temperature-dependent variation trends for samples with different Tb contents, which can be clearly seen in Fig. (3). As shown in Fig. 3(a), the $H_{c\perp}$ value for $x = 25.5\%$ decreases slowly with the increase of temperature when T is below 200 K, above which it drops dramatically. Here $T = 200$ K is the transition point of magnetization compensation temperature (T_{Mcomp}) for the sample of $x = 25.5\%$, i.e. the sample is Co/Ni rich at $T > T_{Mcomp}$ and TbCo rich as $T < T_{Mcomp}$. According to our analyses in the preceding parts, maximum $H_{c\perp}$ should take place at the T_{Mcomp} where magnetic moments are compensated. However, the $H_{c\perp}$ value keeps increasing as T decreases from 200 K to 50 K, we attribute this increase to the enhanced PMA strength of TbCo pinning layer at reduced temperatures. For the $x = 30.0\%$ sample the temperature dependence of $H_{c\perp}$ is similar to that of $x = 25.5\%$ case, except that it has a higher T_{Mcomp} of about 260 K. However, for the sample of $x = 33.0\%$ which has a T_{Mcomp} of RT, the varying trend of $H_{c\perp}$ is distinctly different from the other two samples. Instead of a monotonic slow increase as T decreases from $T_{Mcomp} =$ RT, the $H_{c\perp}$ value firstly decreases and subsequently increases after reaching a minimum at about 200 K. We attribute such behavior to the combined action of enhanced PMA strength and net magnetic moment. The initial decrease of $H_{c\perp}$ originates from the enlarged uncompensated moment of the heterostructure due to the much rapidly increased Tb moment in TbCo layer, whereas with further decreasing temperature the PMA enhancement plays a dominant role which leads to the slow increasing behavior, similar to the varying trend of samples of $x = 25.5\%$ and 30.0% at T < 200 K. Interestingly, as shown in Fig. 3(b), the H_{ex} value at $T = T_{Mcom}$ is always the smallest for all the three samples. The fast increase of H_{ex} with T at $T > T_{Mcomp}$ can be ascribed to the reduced magnetization of TbCo switched layer. Nevertheless, at $T < T_{Mcomp}$ the switching field change of Co/Ni layer is very likely related to the enhanced PMA of TbCo pinning layer.

In addition to the Tb content, the TbCo layer thickness also plays an important role on the magnetization switching of [Co/Ni]$_5$/TbCo heterostructures. Figure 4(a) shows the $H_{c\perp}$ and H_{ex} values for samples with a fixed Tb content of $x = 30.0\%$ but various $Tb_{30}Co_{70}$ layer thicknesses. Three representative out-of-plane magnetic loops of $t = 8.0$, 13.5, and 20 nm, measured by Vibrating Sample Magnetometer (VSM), are inserted in Fig. 4(a). With the increase of $Tb_{30}Co_{70}$ thickness, we find the $H_{c\perp}$ varies also non-monotonically. It firstly increases with increasing t and then begins to decrease at $t = 13.5$ nm, which means that $t \approx 13.5$ nm is the magnetization compensation thickness for the [Co0.28/Ni0.58]$_5$/Tb$_{30}$Co$_{70}$
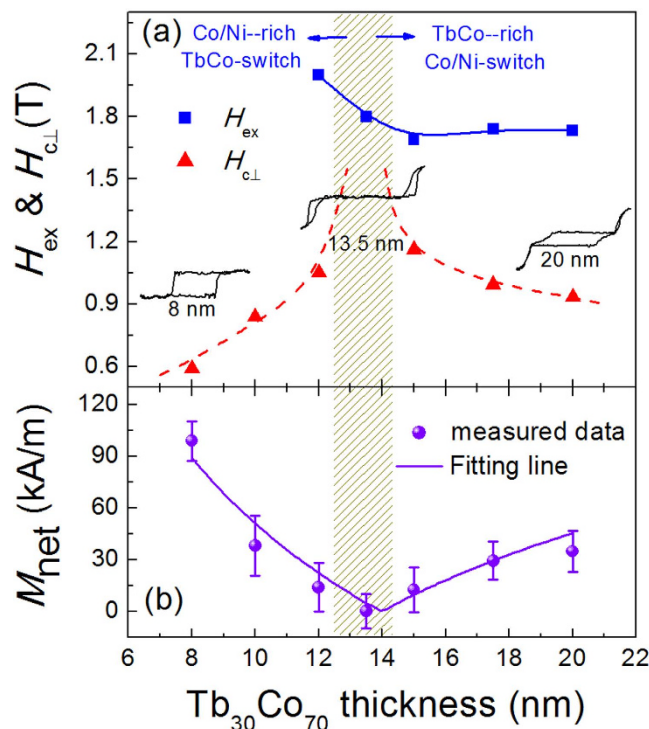
Figure 4. The influence of $Tb_{30}Co_{70}$ thickness on the magnetic properties. (**a**) The perpendicular coercive field $H_{c\perp}$ and exchange coupling field H_{ex}, and (**b**) remanent net magnetization M_{net} as a function of $Tb_{30}Co_{70}$ thickness for samples of $[Co0.28/Ni0.58]_5/$ $Tb_{30}Co_{70}$ (t). Insets: Magnetic hysteresis loops for $t = 8$, 13.5, and 20 nm.

(t) heterostructure. Meanwhile, no central switching loop takes place from the magnetic hysteresis loop of $t = 13.5$ nm sample, confirming that the total net magnetic moment is compensated. Accompanied with the change of $H_{c\perp}$, the exchange coupling field H_{ex} also varies but in a different way. At $t < 13.5$ nm, the sample is Co/Ni rich, so the coupling field comes from the TbCo layer switching, which certainly increases with the decrease of TbCo layer thickness. As soon as t is over 13.5 nm, the Co/Ni layer with fixed magnetization and thickness will be switched. Therefore, owing to the increased PMA of thicker TbCo layer, the H_{ex} exhibits a weak increase. Note that the H_{ex} value for the samples of $t < 12$ nm is not given here because it is far beyond the highest magnetic field of 2.2 T supplied by our VSM. Figure 4 (b) shows the remanent net magnetization (M_{net}) values as a function of $Tb_{30}Co_{70}$ thickness. As expected, starting from the compensation thickness, the M_{net} increases from zero towards both thicker and thinner $Tb_{30}Co_{70}$ layers. By using the following equation of $M_{net} = (M_{s-FM}t_{FM} - M_{s-FI}t_{FI})/(t_{FM} + t_{FI})$, we obtain the Co/Ni magnetization of $M_{s-FM} = 596 \pm 45$ kA/m and $Tb_{30}Co_{70}$ of $M_{s-FI} = 183 \pm 15$ kA/m, which are in good agreement with the measured values (604 kA/m for $[Co0.28/Ni0.58]_5$ and 176 kA/m for $Tb_{30}Co_{70}$). Based on these results, we calculate the interfacial coupling strength J_{ex} is up to 4.4 ± 0.3 mJ/m², such magnitude is comparable to the value found in other exchange-coupled FI/FM structures[12,17], but greatly higher than that of the FM/AFM systems.

Furthermore, we selected 12 nm-thick $Tb_{30}Co_{70}$ as the switching layer and investigated the PMA effect of the FM pinning layer on the H_{ex} and $H_{c\perp}$. The perpendicular anisotropy energy K_p of the FM pinning layer was firstly modulated by changing the repetition number N of the $[Co/Ni]_N$ multilayer. Figure 5(a) shows the $H_{c\perp}$ and H_{ex} of the heterostructure, as well as the effective uniaxial anisotropy energy K_p of the single Co/Ni layer as a function of N for the $[Co/Ni]_N/Tb_{30}Co_{70}$ (12.0) samples. The K_p was calculated according to $K_p = M_sH_k/2$, where H_k is the saturation magnetic field of in-plane magnetic loops. Apparently, the K_p increases monotonically with N due to the increased Co/Ni interfaces. From the maximum $H_{c\perp}$ we can conclude that the magnetization is compensated at N = 4. Therefore, the magnetization of Co/Ni is dominant and the TbCo layer will be switched at N > 4. Although the magnetization and layer thickness of TbCo layer are fixed, we can still see an obvious H_{ex} increase, which can be ascribed to the enhanced K_p of the FM layer. By optimizing the layer structure, we achieved large $H_{c\perp}$ up to 1.31 T and H_{ex} of 2.19 T simultaneously at the N = 4 case, which will be of great importance for practical applications. In addition, the PMA strength of Co/Ni layer was manipulated by tuning the thickness of an additional Co interlayer inserted between the $[Co/Ni]_5$ and $Tb_{30}Co_{70}$ (12.0) layers as well. The interlayer Co thickness t_{Co} is kept below 1.2 nm to ensure the easy axis of Co/Ni along perpendicular
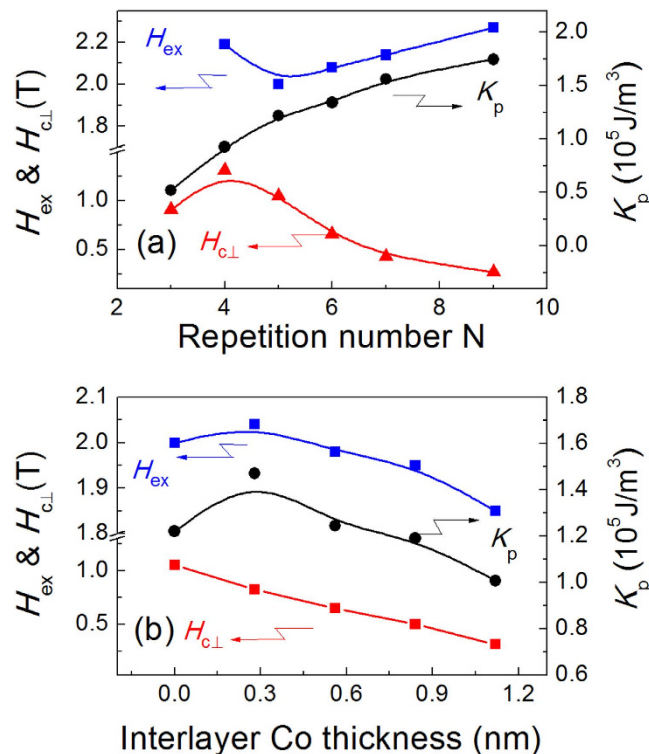
Figure 5. The PMA strength effect on the magnetic properties. Dependences of $H_{c\perp}$, H_{ex}, and magnetic anisotropy energy K_p of the FM layer on (**a**) the repetition number N for the samples of $[Co0.28/Ni0.58]_N/$ $Tb_{30}Co_{70}$ (12) and (**b**) the interlayer Co thickness t_{Co} for the samples of $[Co0.28/Ni0.58]_5/Co(t_{Co})/Tb_{30}Co_{70}$ (12).

direction. A maximum K_p occurs at $t_{Co} = 0.28\,nm$, further increasing t_{Co} will give rise to K_p decrease. Such non-monotonic variation is the result of competition between the interfacial PMA and in-plane shape anisotropy. For this sample structure, the net magnetization is always dominated by [Co/Ni]/Co and increases with t_{Co}, thus leading to the monotonic reduction of $H_{c\perp}$, as shown in Fig. 5(b). Meanwhile, the H_{ex} follows a similar variation trend to the K_p, again demonstrating that the exchange coupling field is strongly dependent on K_p of the pinning layer.

In conclusion, we have investigated the antiferromagnetic exchange coupling interactions and net magnetization switching in perpendicular $[Co/Ni]_N/TbCo$ composite structures. The magnetization compensation composition, compensation thickness of FM or FI layer, as well as compensation temperature for the coupled heterostructures have been clarified. By controlling the magnetization, thickness and PMA strength of the FM and FI layers, a wide range of variation in both net magnetization switching field $H_{c\perp}$ and exchange coupling field H_{ex} are realized. The calculated interfacial coupling strength at RT is as strong as $4.4 \pm 0.3\,mJ/m^2$, leading to a large H_{ex} value even exceeding $3.0\,T$, which is significantly higher than the normal FM/AFM systems. These results offer us valuable information for practical applications in data storage technology and profound understanding of the fundamental exchange coupling mechanism.

Methods

Different series of samples, in a structure of glass/Ta(3)/Cu(3)/$[Co0.28/Ni0.58]_N$/Co (t_{Co})/Tb_xCo_{100-x} (12)/Ta(5) (layer thickness in unit of nm), were deposited sequentially at ambient temperature in a Kurt J. Lesker magnetron sputter system with a base pressure better than 1×10^{-8} Torr. The TbCo alloy layer was fabricated by co-sputtering from pure Tb and Co targets, their relative atomic concentration was controlled by varying the sputtering power of Tb and determined by X-ray Photoelectron Spectroscopy (XPS). Magnetic properties were characterized by Vibrating Sample Magnetometer and Physical Property Measurement System.

References

1. Takano, K., Kodama, R. H, Berkowitz, A. E., Cao, W. & Thomas, G. Interfacial uncompensated antiferromagnetic spins: role in unidirectional anisotropy in polycrystalline $Ni_{81}Fe_{19}(y)/CoO$ bilayers. *Phys. Rev. Lett.* **79,** 1130–1133 (1997).

2. Mishra, S. K. *et al.* Dual behavior of antiferromagnetic uncompensated spins in NiFe/IrMn exchange biased bilayers. *Phys. Rev. B* **81,** 212404 (2010).

3. Sort, J., Baltz, V., Garcia, F., Rodmacq, B. & Dieny, B. Tailoring perpendicular exchange bias in [Pt/Co]-IrMn multilayers. *Phys. Rev. B* **71,** 054411 (2005).

4. Garcia, F., Sort, J., Rodmacq, B., Auffret, S. & Dieny, B. Large anomalous enhancement of perpendicular exchange bias by introduction of a nonmagnetic spacer between the ferromagnetic and antiferromagnetic layers. *Appl. Phys. Lett.* **83,** 3537–3539 (2003).

5. Wu, Q. *et al.* Magnetization reversal asymmetry in [Co/Pt]/CoFe/IrMn multilayers with enhanced perpendicular exchange bias. *J. Appl. Phys.* **113,** 033901 (2013).

6. Lamirand, A. D. *et al.* Robust perpendicular exchange coupling in an ultrathin CoO/PtFe double layer: Strain and spin orientation. *Phys. Rev. B* **88,** 140401(R) (2013).

7. Meiklejohn, W. & Bean, C. P. New magnetic anisotropy. *Phys. Rev.* **102,** 1413–1414 (1956).

8. Li, Z., Zhang, Z., Zhao, H., Ma, B. & Jin, Q. Y. High giant magnetoresistance and thermal annealing effects in perpendicular magnetic [Co/Ni]$_N$-based spin valves. *J. Appl. Phys.* **106,** 013907–013907 (2009).

9. Yuasa, S., Nagahama, T., Fukushima, A., Suzuki, Y. & Ando, K. Giant room-temperature magnetoresistance in single-crystal Fe/MgO/Fe magnetic tunnel junctions. *Nature Mater.* **3,** 868–871 (2004).

10. Chappert, C., Fert, A. & Van Dau, F. N. The emergence of spin electronics in data storage. *Nature Mater.* **6,** 813–823 (2007).

11. Kryder, M. H. *et al.* Heat assisted magnetic recording. *Proc. IEEE* **96,** 1810–1835 (2008).

12. Romer, S. *et al.* Temperature dependence of large exchange-bias in TbFe-Co/Pt. *Appl. Phys. Lett.* **101,** 222404 (2012).

13. Alebrand, S. *et al.* Light-induced magnetization reversal of high-anisotropy TbCo alloy films. *Appl. Phys. Lett.* **101,** 162408 (2012).

14. Mangin, S. *et al.* Engineered materials for all-optical helicity-dependent magnetic switching. *Nature Mater.* **13,** 286–292 (2014).

15. Watson, S. M., Hauet, T., Borchers, J. A., Mangin, S. & Fullerton, E. E. Interfacial magnetic domain wall formation in perpendicular- anisotropy, exchange-spring films. *Appl. Phys. Lett.* **92,** 202507 (2008).

16. Mangin, S. *et al.* Influence of interface exchange coupling in perpendicular anisotropy [Pt/Co]$_{50}$/TbFe bilayers. *Phys. Rev. B* **78,** 024424 (2008).

17. Schubert, C. *et al.* Interfacial exchange coupling in Fe-Tb/[Co/Pt] heterostructures. *Phys. Rev. B* **87,** 054415 (2013).

18. Radu, F., Abrudan, R., Radu, I., Schmitz, D. & Zabel, H. Perpendicular exchange bias in ferrimagnetic spin valves. *Nat. Commun.* **3,** 715 (2012).

19. Gottwald, M. *et al.* Magnetoresistive effects in perpendicularly magnetized Tb-Co alloy based thin films and spin valves. *J. Appl. Phys.* **111,** 083904 (2012).

20. Liao, J., He, H., Zhang, Z., Ma, B. & Jin, Q. Y. Enhanced difference in switching fields for perpendicular magnetic spin valves with a composite [Co/Ni]$_N$TbCo reference layer. *J. Appl. Phys.* **109,** 023907 (2011).

21. Tang, M., Zhang, Z., Zhu, Y., Ma, B. & Jin, Q. Role of TbFe on perpendicular magnetic anisotropy and giant magnetoresistance effect in [Co/Ni]$_N$-based spin valves. *Nano-Micro Lett.* **6,** 359–364 (2014).

22. Mangin, S. *et al.* Current-induced magnetization reversal in nanopillars with perpendicular anisotropy. *Nature Mater.* **5,** 210–215 (2006).

23. Mishra, D., Perumal, A. & Srinivasan, A. High temperature coercive field behavior of Fe–Zr powder. *J. Appl. Phys.* **105,** 07A306 (2009).

24. Mauri, D., Siegmann, H. C., Bagus, P. S. & Kay, E. Simple model for thin ferromagnetic films exchange coupled to an antiferromagnetic substrate. *J. Appl. Phys.* **62,** 3047–3049 (1987).

25. Shimanuki, S., Ichihara, K., Yasuda, N., Ito, K. & Kon, K. Perpendicular magnetic anisotropy in amorphous TbCo sputtered films. *IEEE Transl. J. Magn. Jpn.* **2,** 338–339 (1987).

Acknowledgments

Author Contributions

Z.Z.Z. and Q.Y.J. conceived and supervised the study. M.H.T. fabricated the samples and performed the VSM and XPS measurements. S.Y.T. and J.W. performed the PPMS experiments. Z.Z.Z. and M.H.T. analyzed the data and wrote the paper. All authors discussed the results and commented on the manuscript.

Additional Information

Competing financial interests: The authors declare no competing financial interests.

How to cite this article: Tang, M. H. *et al.* Interfacial exchange coupling and magnetization reversal in perpendicular [Co/Ni]$_N$ /TbCo composite structures. *Sci. Rep.* **5**, 10863; doi: 10.1038/srep10863 (2015).